

$$M_Y = N_Z L_X - N_X L_Z \quad (14)$$

$$M_Z = N_X L_Y - N_Y L_X \quad (15)$$

Next an equivalent  $R$  matrix using homogeneous coordinate transformation equations is developed by combining the three rotational matrices in the references. As mentioned previously, the order of combination is important. If they are combined as roll times pitch and then times yaw, the following matrix is formed:

$$\begin{bmatrix} [\cos\alpha \cos\beta] & [\cos\alpha \sin\beta] & [-\sin\alpha] \\ [(\sin\gamma \sin\alpha \cos\beta) - \cos\gamma \sin\beta] & [(\sin\gamma \sin\alpha \sin\beta) + \cos\gamma \cos\beta] & [\sin\gamma \cos\alpha] \\ [(\cos\gamma \sin\alpha \cos\beta) + \sin\gamma \sin\beta] & [(\cos\gamma \sin\alpha \sin\beta) - \sin\gamma \cos\beta] & [\cos\gamma \cos\alpha] \end{bmatrix} \quad (16)$$

Equating terms to the matrix in Eq. (1) gives nine equations in three unknown variables. From these we can determine that

$$\alpha = \sin^{-1}(-L_Z) \quad (17)$$

$$\beta = \cos^{-1}(L_X/\cos\alpha) = \sin^{-1}(L_Y/\cos\alpha) \quad (18)$$

$$\gamma = \sin^{-1}(M_Z/\cos\alpha) = \cos^{-1}(N_Z/\cos\alpha) \quad (19)$$

Either of the two possible values of  $\alpha$  are correct.  $\beta$  and  $\gamma$  are uniquely determined once  $\alpha$  is selected.

The required  $x_I$ ,  $y_I$ , and  $z_I$  local axis origin values are the coordinates of  $P_I$ , which were subtracted from the coordinates of  $P_2$  and  $P_3$  to get a pure rotation problem prior to calculation of the  $L$ ,  $M$ , and  $N$  terms.

There is a trivial case to consider. If  $\cos\alpha = 0$ , there is no solution by this method. This occurs when the local  $X$  axis aligns with the global  $Z$  axis. This is indicated when  $|L_Z| = 1$  and  $L_X = L_Y = 0$ , thus  $\alpha = (-L_Z)\pi/2$ .

As we have selected rotation order of roll, then pitch, then yaw, it follows that when pitch is  $(-\pi/2)$ , the roll and yaw must sum to the total angle  $\theta$  between the local  $Y$  axis and the global  $Y$  axis. If the pitch is  $+\pi/2$  the yaw has negative sign, thus

$$\beta - L_Z\gamma = \theta \quad (20)$$

where

$$\theta = \sin^{-1}(-M_X) = \cos^{-1}(M_Y) \quad (21)$$

Any combination of  $\beta$  and  $\gamma$  meeting the equations is correct.

### Application of the Inverse Procedure

We have now identified a procedure for determining  $x_I$ ,  $y_I$ ,  $z_I$ , roll, pitch, and yaw for a local axis system given three points; the local axis system origin  $P_I$ , a point  $P_2$  on the desired local  $X'$  axis, and a point  $P_3$  on the desired local  $X'Y'$  plane.

Applications of this procedure now will be described. The most direct application is to allow the designer to specify that a component will go from "here to there" by input of three points. The first point is "here" and becomes  $P_I$  in the preceding calculations. The second point is "there" and becomes  $P_2$ . The third point,  $P_3$ , specifies only the component roll about the  $X$  axis by defining the  $X'Y'$  plane. This capability is shown in Figs. 2 and 3.

Figure 2 shows a typical design problem. A wing strut is required extending from point  $P_I$  to point  $P_2$ , and is oriented such that the airfoil streamwise direction ( $Y$  axis) is approximately parallel to the global  $X$  axis.  $P_3$  is coincident with  $P_2$  in rear view and forward of  $P_2$  in top view, thus orienting

the  $X-Y$  plane properly. Note the initial strut location which is irrelevant to our solution.

Figure 3 shows the resulting strut location. The calculated values obtained in this example are  $x_I = 70.35$ ,  $y_I = 9.07$ ,  $z_I = -9.28$ , roll = 0.7 deg, pitch = 18.8 deg, and yaw = 87.9 deg.

A second utilization of this procedure for determining the local axis system values permits component rotations in the global axis system regardless of the original orientation of the local axis system.

This can be implemented using the preceding equations by a simple trick. We take three arbitrary points in the local axis system, convert them to global coordinates, rotate them in the global system, and then use the given procedure to find the new local axis system  $x_I$ ,  $y_I$ ,  $z_I$ , roll, pitch, and yaw. To simplify matters, the three local axis system points selected are  $P_I = (0, 0, 0)$ ,  $P_2 = (1, 0, 0)$ , and  $P_3 = (0, 1, 0)$ .

Trunnion axis rotations can be implemented in a similar fashion. This and the related problem of trunnion axis location are detailed in Ref. 4.

### References

- <sup>1</sup>Giloi, W. *Interactive Computer Graphics*. Prentice Hall, Englewood Cliffs, N.J., 1978.
- <sup>2</sup>Foley, J. and Van Dam, A. *Fundamentals of Interactive Computer Graphics*. Addison-Wesley Publishing Co., Reading, Mass., 1982.
- <sup>3</sup>Faux, I. D. and Pratt, M. J. *Computational Geometry for Design and Manufacture*. John Wiley & Sons, New York, 1979.
- <sup>4</sup>Raymer, D. P., Maier, R. A., and Killian, M. J. *Conceptual Kinematic Design Using Homogeneous Coordinate Transformations*. AIAA Paper 83-2460, Oct. 1983.

## A Method for Measuring Skin Friction Drag on a Flat Plate in Contaminated Gas Flows

R. B. Oetting\* and G. K. Patterson†  
University of Missouri-Rolla, Rolla, Missouri

### Introduction

THE most straightforward way to measure drag on a surface immersed in a fluid flow is by direct measurement of the force on the exposed surface.<sup>1</sup> This usually involves replacing a portion of the surface with an imbedded sensor surface, generally about 0.5 to 1 in. in diameter (some noncircular sensors have been used). The surface is directly connected to a small force transducer beneath the plate. It is possible to achieve good results with these sensors, but care must be taken in their installation<sup>2</sup> to avoid misalignment of the surfaces and binding between the sensor surface and the surrounding plate surface.

An alternate method of determining surface drag is through indirect methods based on similarity arguments and/or cer-

Received Feb. 15, 1984. Copyright © American Institute of Aeronautics and Astronautics, Inc. 1984. All rights reserved.

\*Professor, Department of Mechanical and Aerospace Engineering Associate Fellow AIAA.

†Professor, Department of Chemical Engineering; currently at University of Arizona.

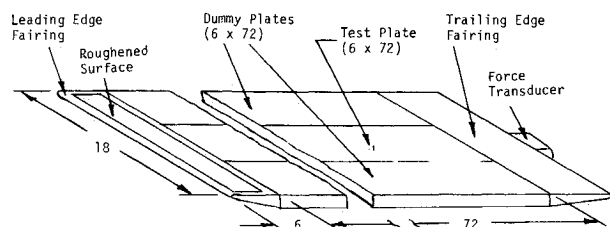


Fig 1 Drag plate configuration (all dimensions in inches)

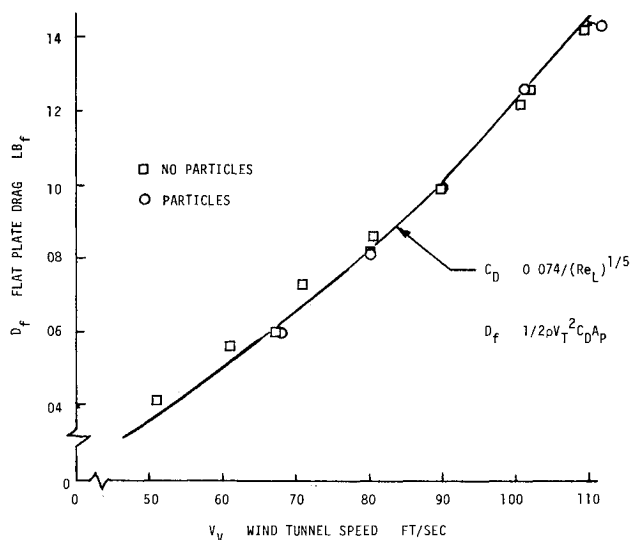


Fig 2 Flat plate drag comparisons

tain assumptions about the velocity profile and turbulence level in the surface boundary layer. In this broad category of drag determination, the method most easily understood involves the measurement of the velocity profile of the boundary layer, usually with a hot wire anemometer. Once the velocity profile is established it is possible to determine the surface friction coefficient by techniques such as the logarithmic law of the wall presented by Clauser.<sup>3</sup>

Neither the method utilizing the embedded sensor surface, nor an indirect method involving the measurement of the surface boundary layer velocity profile, is adequate when the fluid flowfield is contaminated with particles. Particles as small as 50  $\mu\text{m}$  diameter suspended in the flow would interfere with the function of both the embedded sensor and the hot wire probe. The technique of skin friction drag measurement presented here was developed to overcome the problem of suspended particles in the fluid flow. This activity was part of a larger project<sup>4</sup> to investigate the potential for drag reduction of suspended particles in the developing boundary layer on a flat plate. The key to the success of the present technique of measuring the flat plate surface drag is the suspension of the test plate on air bearings.

### Apparatus

The flat plate arrangement is shown in Fig 1. The 0.25 in thick aluminum test plate (6 in wide  $\times$  72 in long) is located between two dummy plates of the same size and material. A gap of about 0.02 in separates the test plate from the dummy side plates and the leading and trailing edge fairings. The leading edge fairing<sup>5</sup> provides some flow conditioning and the rear fairing provides trailing edge streamlining and a housing for the Revere model UMP1 0 005 A load cell transducer. Side rails and a lower plate support the dummy plates, test plate air bearings and force transducer. This arrangement also protects the air bearings and force transducer from particle contamination from the underside of the test arrangement.

The air bearing arrangement for the test plate suspension includes six horizontal bearings for plate support, with four

more vertical bearings for plate alignment. The horizontal air bearings are located in pairs equally spaced along the length of the test plate. Vertical alignment air bearings are located in pairs equidistant between the front and center, and center and rear horizontal air bearings. This arrangement allows for good plate support with the six horizontal air bearings, and the ability to control the gap separating the test plate from the dummy plates using the four adjustable vertical air bearings.

The experiments were carried out in the University of Missouri Rolla Subsonic Wind Tunnel, a closed circuit atmospheric tunnel with a test section 32 in high  $\times$  48 in wide  $\times$  11 ft long. Low turbulence (on the order of 0.2%) and good flow direction control are obtained by a combination of features, including two screens in the stilling chamber, 9:1 stilling chamber to test section contraction ratio, feedback command control of fan speed, and a 6.5 deg maximum diffuser angle. Tests were run at tunnel speeds up to 150 ft/s.

Particles were injected through a spread nozzle (6 in wide  $\times$  1/16 in deep) at a position in the inlet contraction upstream of the test plate to minimize flowfield interference. Oxides of aluminum and iron particles were used, ranging in size from 20 to 150  $\mu\text{m}$ . Particle densities were as high as 0.3 lb of particle per pound of air.

### Results and Discussion

Comparison of the experimental drag measurements with theory for the 6 in wide  $\times$  72 in long (3 ft<sup>2</sup>) test plate is shown in Fig 2. The experimental measurements are compared with the drag force calculated using the equation<sup>6</sup>

$$C_D = 0.074 / (Re_L)^{1/5}$$

for a turbulent boundary layer starting at the test plate leading edge. A roughened surface on the leading edge fairing (see Fig 1) causes the boundary layer to trip and become a turbulent boundary layer before reaching the test plate leading edge. This was confirmed through boundary layer velocity profile measurements using a hot wire anemometer with no particle injection into the flowfield. A turbulent boundary layer exists over the entire test plate for tunnel speeds above 50 ft/s.

The results of this study indicate that the measurement of drag on a flat plate in a particle contaminated airflow can be readily made utilizing a system which supports the test plate on air bearings. Adjustment of the air bearing support system is easily made to properly align the plate to prevent interference with the surrounding support system.

### Acknowledgments

This work was performed as part of a research project supported through the NASA Langley Research Center, NASA NSG 1452. The authors would like to acknowledge the contribution of Walter A. Lounsbery, aerospace engineering graduate student who was instrumental in organizing and performing the experiments.

### References

- <sup>1</sup>Dhawan, S. Direct Measurement of Skin Friction. NACA Rept 1121, 1952.
- <sup>2</sup>Issa, R. K. and Lockwood, F. C. Experimental Study of Error Sources in Skin Friction Balance Measurements. *Journal of Fluid Mechanics*, Vol 99, No 1, March 1977, pp 197-204.
- <sup>3</sup>Clauser, F. H. Turbulent Boundary Layers in Adverse Pressure Gradients. *Journal of the Aeronautical Sciences*, Vol 21, No 2, Feb 1954, pp 91-108.
- <sup>4</sup>Patterson, G. K., Oetting, R. B., Anderson, R. A., and James, W. J. Study of Gas-Solid Airflow Over a Flat Plate, Final Tech Rept. NASA NSG 1452, University of Missouri Rolla, Rolla, Mo, Jan 1983.
- <sup>5</sup>Davis, M. R. Design of Flat Plate Leading Edges to Avoid Separation. *AIAA Journal*, Vol 18, May 1980, pp 598-600.
- <sup>6</sup>Schlichting, H. *Boundary Layer Theory*, 4th Ed. McGraw-Hill Book Co., New York, 1960, pp 536-539.